Superhydrophobic Surfaces | Hot Paper

Deutsche Ausgabe: DOI: 10.1002/ange.201500137
Internationale Ausgabe: DOI: 10.1002/anie.201500137

Fabrication of Condensate Microdrop Self-Propelling Porous Films of Cerium Oxide Nanoparticles on Copper Surfaces**

*Yuting Luo, Juan Li, Jie Zhu, Ye Zhao, and Xuefeng Gao**

Abstract: *Condensate microdrop self-propelling (CMDSP) surfaces have attracted intensive interest. However, it is still challenging to form metal-based CMDSP surfaces. We design and fabricate a type of copper-based CMDSP porous nanoparticle film. An electrodeposition method based on control over the preferential crystal growth of isotropic nanoparticles and synergistic utilization of tiny hydrogen bubbles as pore-making templates is adopted for the in situ growth of cerium oxide porous nanoparticle films on copper surfaces. After characterizing their microscopic morphology, crystal structure and surface chemistry, we explore their CMDSP properties. The nanostructure can realize the efficient ejection of condensate microdrops with sizes below 50 μm.*

Condensate microdrop self-propelling (CMDSP) surfaces have attracted intensive interest due to their values in basic research and technological innovations, such as moisture self-cleaning,[1] anti-frosting,[2–4] power generation,[5–7] and enhancing condensation heat transfer for high-efficiency energy utilization and thermal management.[8–12] Differing from the gravity-driven shedding-off mode of macroscopic water drops on conventional superhydrophobic surfaces,[13] the efficient self-propelling of condensed microdrops can be realized through their coalescence-released excess surface energy, without requiring external forces, such as gravity and steam shear force.[14] To date, many efforts have been made to obtain CMDSP by the creation of arrays of nanostructures (i.e., nanoscale wires, needles, cones, and sheets) or hierarchical structures followed by low-surface-energy chemistry.[2–7,10–23] However, it is still challenging to form metal-based CMDSP films, which are rarely studied despite their important value in daily life and industry processes. In terms of low-cost large-area nanoprocessing and equipment accessibility, wet-chemical nanosynthesis methods[3–6,10,15–19] are more suitable for in situ fabrication of CMDSP films on metal surfaces than top-down nanofabrication methods.[2,7,11,20–23] Therefore, it is significant to explore novel metal-based CMDSP nanostructures and wet-chemistry processing methods.

It has been reported that ensuring an extremely low solid–liquid interface adhesion and avoiding the penetration of moisture by fine surface nanoengineering are the keys to realizing CMDSP.[24–28] Based on this principle, we propose that metal-based CMDSP surfaces may be formed by using hydrophobic porous nanoparticle structures. To verify this idea we carried out the in situ growth of copper-based cerium oxide porous nanoparticle films by electrodeposition based on control over the preferential growth of isotropic nanoparticles and synergistic utilization of tiny hydrogen bubbles released from the hydrogen-evolution reaction (HER) as pore-making templates. The microscopic morphology, chemical compositions, and crystal structure of the sample surface are systematically characterized by high-resolution scanning electronic microscopy (SEM), atomic force spectroscopy (AFM), X-ray photoelectron spectroscopy (XPS) and X-ray diffraction (XRD). As expected, the nanostructure films indeed show CMDSP after hydrophobicization.

To realize the desired CMDSP, the dissipation of coalescence released excess surface energy caused by solid–liquid adhesion must be minimized.[24,25] According to our recent work,[29] we can reasonably predict that the porous nanoparticle film should have extremely low solid–liquid interface adhesion. Generally, larger pores (or cavities) help reduce both solid–liquid contact area and interface adhesion. However, pores that are too large inevitably risk allowing the penetration of moisture.[26–28] This is why lotus leaves with larger characteristic length (ca. 20 μm) of valleys can show low adhesion of macroscopic water drops but highly adhesion of microdrops.[28] So, the pores should be restricted at the submicrometer scale to avoid the penetration of moisture. As shown in the left of Figure 1 a, water molecules are prone to self-aggregate into clusters above the subcooled substrate (with surface temperature lower than the ambient saturation temperature),[30] absorb at the near-surface nanoparticle sites in a spatially random fashion and rapidly grow by preferential absorption of ambient moisture. The tiny condensate drops formed can easily bridge between the tops of the nanoparticle walls of submicrometer-size pores (Figure 1 a). Owing to their very strong capillary force, the menisci of the drops prevent the downward penetration of the condensate into the micropores. As a result, these suspended condensate microdrops can eject themselves ("self-depart" in a "self-jumping" mode) by their mutual coalescence, as shown in the right panel of Figure 1 a. The next issue is how to achieve the in situ growth of porous nanoparticle films on the copper surface using

[*] Y. Luo, Dr. J. Li, J. Zhu, Y. Zhao, Prof. X. Gao
Advanced Thermal Nanomaterials and Devices Research Group, Nanobionic Division, Suzhou Institute of Nano-Tech and Nano-Bionics
Chinese Academy of Sciences, Suzhou 215123 (China)
E-mail: xfgao2007@sinano.ac.cn
Y. Luo
School of Environment and Chemical Engineering
Shanghai University, Shanghai 200444 (China)

[**] This work was supported by the National Basic Research Program of China (2012CB933200), Key Research Program of the Chinese Academy of Sciences (KJZD-EW-M01) and Suzhou Institute of Nano-Tech and Nano-Bionics, Chinese Academy of Sciences.

Supporting information for this article is available on the WWW under http://dx.doi.org/10.1002/anie.201500137.

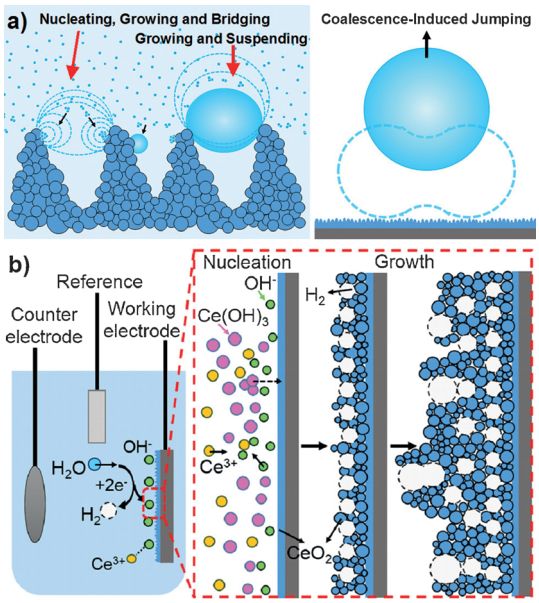

Figure 1. a) Schematic diagrams of utilizing rugged, porous, nanoparticle films to endow copper surfaces with a condensate microdrop self-propelling function. b) Schematic diagrams of synthesizing porous films of cerium oxide nanoparticles by the control of the preferential growth of isotropic nanoparticles and the synergistic utilization of tiny bubbles, released by the hydrogen-evolution reaction, as pore-making templates. Sky blue H_2O, green OH^- ions, orange Ce^{3+} ions, pink $Ce(OH)_3$, blue CeO_2, white H_2.

a facile, cheap, and scalable wet-chemical method and verify their utility.

It has been reported that electrodeposited cerium oxide films can be used as a type of eco-friendly metal-based anticorrosion coating.[31] However, there is no report about three-dimensional, rugged, porous cerium oxide nanoparticle films and their use for studying the CMDSP function. Other nanostructures have been prepared for investigations in fields, such as, catalysis, luminescent devices, biological labeling.[32–34] To realize the in situ growth of porous films of cerium oxide nanoparticles on the copper surface, we propose a strategy of controlling electrochemical parameters to induce the preferential growth of isotropic nanoparticles and simultaneously utilizing tiny hydrogen bubbles as pore-making templates, as shown in Figure 1 b. A three-electrode system is adopted, in which the working electrode is a copper plate, the counter electrode is Pt foil, and the reference electrode is Ag/AgCl. In principle, $Ce(OH)_3$ "gel" can rapidly form nearby the copper surface at the initial reaction stage,[35] where the OH^- ions released by water electrolysis react with Ce^{3+} ions. Then, the oxidation and dehydration of $Ce(OH)_3$ can induce a super-thin CeO_2 film that uniformly deposits on the copper surface. To promote the switch of the $Ce(OH)_3$ intermediate into the isotropic CeO_2 nanoparticles, electrochemical parameters (Ce^{3+} and NH_4^+ ion concentration and current density) must be controlled to inhibit anisotropic crystal growth.[32] Meanwhile, the reduction of water can slowly release numerous tiny hydrogen bubbles, which may be used as dynamic pore-making templates for the growth of porous nanoparticle films.[33]

Our studies verify that this strategy indeed can control the in situ growth of cerium oxide nanoparticle porous films on copper surfaces. Very recently, Tong et al.[34] achieved the controllable fabrication of cerium oxide nanorods (or nanowires) on copper surfaces by cathodic electrodeposition in the aqueous solution of 0.01 M $Ce(NO_3)_3$, 0.1 M NH_4Cl, and 0.05 M KCl at a current density of 0.44 mA cm^{-2} (or 0.88 mA cm^{-2}) at 70 °C for 2 h. Interestingly, by reducing the concentration of Ce^{3+} and NH_4^+ to be 0.003 M and 0.03 M and increasing the current density to 1.0 mA cm^{-2}, we can easily achieve the in situ growth of porous nanoparticle films, which only requires 20 min. Figure 2 a shows the typical optical image of a copper plate after electrodeposition. The sample surface appears rather smooth and light pink. However, the sample

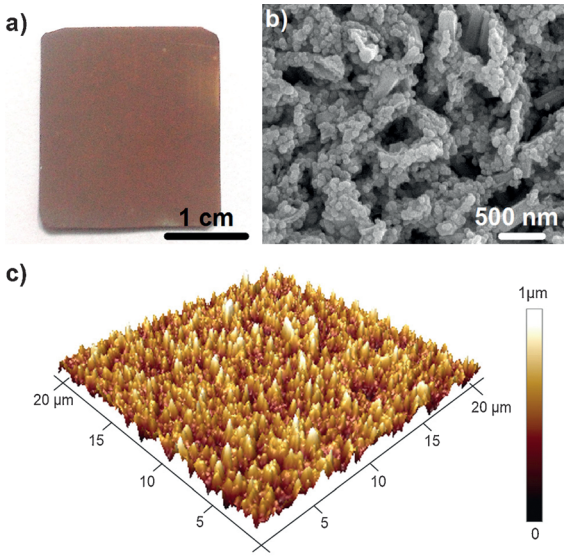

Figure 2. a) Typical optical image, b) top-view SEM image, and c) 3D AFM image of a copper plate covered with electrodeposited porous nanoparticle film.

surface shows three-dimensional rugged features under the SEM (Figure 2 b). Evidently, there are a large number of irregular submicrometer-scale pores distributed randomly inside the rugged nanoparticle films. The diameters of nanoparticles and micropores are in the range of 50–90 nm and 350–850 nm, respectively. Note that a trace of nanorods inevitably exists in the electrodeposited films, which may be ascribed to uneven distribution of local current density during electrodeposition. Figure 2 c offers a typical AFM image of electrodeposited porous nanoparticle films. Clearly, the rugged nanoparticle protrusions and randomly distributed small-scale micropores can effectively reduce the liquid–solid contact area and interface adhesion compared to the flat untreated copper surfaces after hydrophobicization.[29]

Subsequently, we characterized the chemical components and crystal structure of the nanoparticle porous films by the combined use of XRD and XPS. The XRD pattern is shown in Figure 3 a. The four diffraction peaks near 28.7°, 33.3°, 47.8°, and 56.8° are in accordance with diffractions of CeO_2 crystal face (111), (200), (220), and (311), which can be indexed as

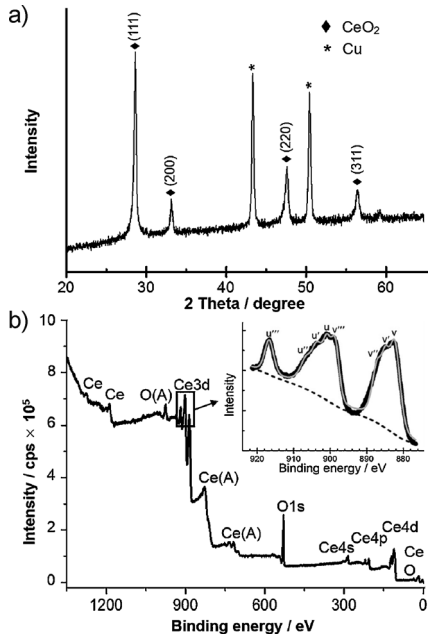

Figure 3. Typical XRD pattern (a) and XPS spectra (b) of the copper-based cerium oxide porous nanoparticle films. Inset: the Ce 3d spectra.

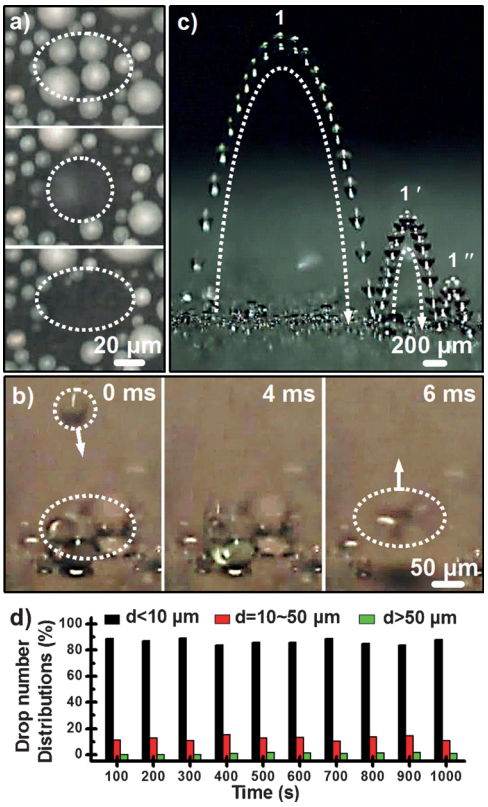

Figure 4. Typical time-lapse optical images showing the self-propelling of condensate microdrops by their mutual coalescence (highlighted by dotted line) trigged by quasi-static growth (a) and dynamic impact (b). c) An overlapped optical image showing a continuous self-propelled jumping event. d) Drop number distributions of condensate microdrops with diameters (d) of <10, 10–50, and >50 μm against time. The samples are placed on a horizontal cooling stage with substrate temperature of approximately 2 °C, ambient temperature approximately 25 °C and relative humidity approximately 90 %.

fluorite cubic structure of CeO_2 (JCPDF#65-2975) with lattice constant $a = 0.5411$ nm. Note that Cu peaks come from the substrate. It appears that the nanoparticle film is made of pure CeO_2. In view of the inherent co-existence of Ce^{4+} and Ce^{3+}, their surface chemistry is further characterized by XPS, as shown in Figure 3b. In the spectrum, only Ce and O are detected. To analyze the chemical state of Ce element, the XPS spectrum of the Ce 3d core level can be fitted into eight components,[36] as shown in the inset of Figure 3b. The peaks labeled as u, u″, u‴, V, V″ and V‴ are those of Ce^{4+} state, while the u′ and V′ are the characteristic peaks of Ce^{3+} state. Evidently, the as-synthesized CeO_2 porous nanoparticle films are mixed with a trace of Ce_2O_3. Note that, differing from the previous reports,[33,34] we can obtain a new type of cerium oxide nanoparticle porous structure in a short reaction time using similar electrodeposition methods but different electrochemical parameters.

Our studies indicate that the cerium oxide nanoparticle porous films have the desired CMDSP function after fluorosilane modification. Figure 4a shows representative optical top views of the instant self-expulsion process of condensate microdrops on the sample surface. It is evident that the in-plane coalescence of adjacent microdrops, caused by their direct condensation growth, can trigger the out-of-plane jumping of the merged microdrop. In addition, these ejected microdrops can fall back to the sample surface and trigger impact-induced self-propelling events, as shown in Figure 4b. This CMDSP mode differs from that caused by the quasi-static growth and can greatly reduce the residence period of microdrops. On the other hand, the continuous jumping events take place frequently on the sample surface (Figure 4c). To quantify the self-removal ability of microdrops on the sample surface, we conducted statistical analyses into drop number distribution of residence microdrops with diameters (d) of $d<10$, 10–50, and $d>50$ μm (Figure 4d). The microdrops with $d<10$ μm account for approximately 90 % and have a slight fluctuation with the time; the microdrops with $d = 10$–50 μm account for around 10 %; the microdrops with $d>50$ μm almost equal to zero. Accordingly, the porous nanoparticle film can realize the efficient self-removal of small-scale condensate microdrops, especially those with the sizes below 50 μm.

In conclusion, we design and fabricate a type of copper-based cerium oxide porous nanoparticle films with the desired CMDSP function. This work helps develop metal-based CMDSP surfaces for moisture self-cleaning, anti-frosting, power generation, enhancing condensation heat transfer and conventional superhydrophobicity applications with regard to macroscopic droplets.[1–12] Firstly, a porous, inorganic nanoparticle-based structure is more suitable for metal-based functional coatings, compared with arrays of nanowires and nanoneedles that are vulnerable to mechanical damage. Such an inorganic nanoparticle film is very robust on the copper substrate, which can be demonstrated by multiple bending of the film-coated substrate without impact on the surface

superhydrophobicity performance (see Movie S1 in the Supporting Information). Secondly, our method is facile, inexpensive, scalable, and promising to be evolved into be practical metal-based surface nanoengineering technologies. In principle, it may be suitable for any metal substrate. In addition, we found that such cerium oxide nanoparticle porous films can become highly hydrophobic by long-term airborne hydrocarbon absorption[37] (the related data will be reported elsewhere).

Experimental Section

Material fabrication: A cerium oxide nanoparticle porous film can be grown on the copper surface by facile electrochemical deposition. To remove the surface oxide layer and contaminants, copper plates (with size of $25 \times 25 \times 0.2\ mm^3$) were mechanically polished and ultrasonically rinsed in acetone, ethanol, and deionized water for 5 min, each. After nitrogen drying, the back of the Cu plates was protected with insulating tape. A three-electrode system was used, where a Cu plate is the working electrode, a Pt foil the counter electrode, and Ag/AgCl as the reference electrode. The electrodeposition reaction was performed in an aqueous solution of 0.003 M $Ce(NO)_3$, 0.03 M NH_4Cl, and 0.015 M KCl at current density of $1.0\ mA\,cm^{-2}$ at 70 °C for 20 min. The electrodeposited Cu plates were treated by ethanol rinsing, nitrogen drying, and heating at 80 °C overnight, respectively. Finally, the samples were placed, together with a beaker containing 10 μL heptadecafluorodecyltrimethoxysilane liquid, into a sealed glass container and then heated for 2 h at 120 °C.

Characterization: The surface morphologies of electrodeposited copper plates were studied by scanning electronic microscope (FEI Quanta250 FEG, USA) and atomic force microscopy (Bruker Dimension Icon, Germany). The crystalline phase of the samples was analyzed by powder X-ray diffraction using $Cu_{K\alpha}$ radiation (Bruker D8 advance, Germany). The chemical composition and chemical state of the sample surface were analyzed by X-ray photoelectron spectroscopy (Thermo Scientific ESCALAB 250Xi, USA). A high-speed microscopic imaging system (Keyence VW-900, Japan) was used for studying dynamic condensation behaviors of the sample surfaces under magnification $\times 30 \approx \times 1000$ with frame rates of 30–4000 fps. The samples were fastened on a horizontally placed cooling stage (ca. 2 °C) in a controlled environment of ambient temperature ca. 25 °C and relative humidity ca. 90 %.

Keywords: cerium oxides · condensate microdrop self-propelling · nanoparticle films · porous materials · superhydrophobic surfaces

How to cite: *Angew. Chem. Int. Ed.* **2015**, *54*, 4876–4879
Angew. Chem. **2015**, *127*, 4958–4961

[1] K. M. Wisdom, J. A. Watson, X. Qu, F. Liu, G. S. Watson, C.-H. Chen, *Proc. Natl. Acad. Sci. USA* **2013**, *110*, 7992.
[2] X. Chen, R. Ma, H. Zhou, X. Zhou, L. Che, S. Yao, Z. Wang, *Sci. Rep.* **2013**, *3*, 2515.
[3] J. Lv, Y. Song, L. Jiang, J. Wang, *ACS Nano* **2014**, *8*, 3152.
[4] Q. Xu, J. Li, J. Tian, J. Zhu, X. Gao, *ACS Appl. Mater. Interfaces* **2014**, *6*, 8976.
[5] N. Miljkovic, D. J. Preston, R. Enright, E. N. Wang, *Nat. Commun.* **2013**, *4*, 2517.
[6] N. Miljkovic, D. J. Preston, R. Enright, E. N. Wang, *Appl. Phys. Lett.* **2014**, *105*, 013111.
[7] N. Miljkovic, D. J. Preston, R. Enright, E. N. Wang, *ACS Nano* **2013**, *7*, 11043.
[8] R. Enright, N. Miljkovic, J. L. Alvarado, K. Kim, J. W. Rose, *Nanosc. Microsc. Therm.* **2014**, *18*, 223.
[9] N. Miljkovic, E. N. Wang, *MRS Bull.* **2013**, *38*, 397.
[10] N. Miljkovic, R. Enright, Y. Nam, K. Lopez, N. Dou, J. Sack, E. N. Wang, *Nano Lett.* **2013**, *13*, 179.
[11] Y. Hou, M. Yu, X. Chen, Z. Wang, S. Yao, *ACS Nano* **2015**, *9*, 71.
[12] J. B. Boreyko, Y. Zhao, C.-H. Chen, *Appl. Phys. Lett.* **2011**, *99*, 234105.
[13] Y. Tian, B. Su, L. Jiang, *Adv. Mater.* **2014**, *26*, 6872.
[14] J. B. Boreyko, C.-H. Chen, *Phys. Rev. Lett.* **2009**, *103*, 184501.
[15] R. Enright, N. Miljkovic, N. Dou, Y. Nam, E. N. Wang, *J. Heat Transfer* **2013**, *135*, 091304.
[16] C. Dietz, K. Rykaczewski, A. Fedorov, Y. Joshi, *Appl. Phys. Lett.* **2010**, *97*, 033104.
[17] J. Feng, Y. Pang, Z. Qin, R. Ma, S. Yao, *ACS Appl. Mater. Interfaces* **2012**, *4*, 6618.
[18] J. Feng, Z. Qin, S. Yao, *Langmuir* **2012**, *28*, 6067.
[19] M. He, Q. Zhang, X. Zeng, D. Cui, J. Chen, H. Li, J. Wang, Y. Song, *Adv. Mater.* **2013**, *25*, 2291.
[20] K. Rykaczewski, A. T. Paxson, S. Anand, X. Chen, Z. Wang, K. K. Varanasi, *Langmuir* **2013**, *29*, 881.
[21] C.-H. Chen, Q. Cai, C. Tsai, C.-L. Chen, G. Xiong, Y. Yu, I. Ren, *Appl. Phys. Lett.* **2007**, *90*, 173108.
[22] C. Dorrer, J. Rühe, *Adv. Mater.* **2008**, *20*, 159.
[23] X. Chen, J. Wu, R. Ma, M. Hua, N. Koratkar, S. Yao, Z. Wang, *Adv. Funct. Mater.* **2011**, *21*, 4617.
[24] J. Tian, J. Zhu, H.-Y. Guo, J. Li, X.-Q. Feng, X. Gao, *J. Phys. Chem. Lett.* **2014**, *5*, 2084.
[25] M. He, X. Zhou, X. Zeng, D. Cui, Q. Zhang, J. Chen, H. Li, J. Wang, Z. Cao, Y. Song, L. Jiang, *Soft Matter* **2012**, *8*, 6680.
[26] K. A. Wier, T. J. McCarthy, *Langmuir* **2006**, *22*, 2433.
[27] C. Dorrer, J. Rühe, *Langmuir* **2007**, *23*, 3820.
[28] Y. Zheng, D. Han, J. Zhai, L. Jiang, *Appl. Phys. Lett.* **2008**, *92*, 084106.
[29] Y. Lai, X. Gao, H. Zhuang, J. Huang, C. Lin, L. Jiang, *Adv. Mater.* **2009**, *21*, 3799.
[30] T. Song, Z. Lan, X. Ma, T. Bai, *Int. J. Therm. Sci.* **2009**, *48*, 2228.
[31] Y. Hamlaoui, F. Pedraza, C. Remazeilles, S. Cohendoz, C. Rébéré, L. Tifouti, J. Creus, *Mater. Chem. Phys.* **2009**, *113*, 650.
[32] H. Mai, L. Sun, Y. Zhang, R. Si, W. Feng, H. Zhang, H. Liu, C. Yan, *J. Phys. Chem. B* **2005**, *109*, 24380.
[33] G.-R. Li, D.-L. Qu, X.-L. Yu, Y.-X. Tong, *Langmuir* **2008**, *24*, 4254.
[34] C. Zhang, X.-Y. Zhang, Y.-C. Wang, S.-L. Xie, Y. Liu, X.-H. Lu, Y.-X. Tong, *New J. Chem.* **2014**, *38*, 2581.
[35] T. D. Golden, A. Q. Wang, *J. Electrochem. Soc.* **2003**, *150*, C621.
[36] P. Burroughs, A. Hamnett, A. F. Orchard, G. Thornton, *J. Chem. Soc. Dalton Trans.* **1976**, *17*, 1686.
[37] D. J. Preston, N. Miljkovic, J. Sack, R. Enright, J. Queeney, E. N. Wang, *Appl. Phys. Lett.* **2014**, *105*, 011601.

Received: January 7, 2015
Published online: February 18, 2015

